We are IntechOpen,
the world's leading publisher of
Open Access books
Built by scientists, for scientists

6,900
Open access books available

185,000
International authors and editors

200M
Downloads

Our authors are among the

154
Countries delivered to

TOP 1%
most cited scientists

12.2%
Contributors from top 500 universities

BOOK CITATION INDEX
CLARIVATE ANALYTICS
INDEXED

WEB OF SCIENCE™

Selection of our books indexed in the Book Citation Index
in Web of Science™ Core Collection (BKCI)

Interested in publishing with us?
Contact book.department@intechopen.com

Switched Reluctance Motor Drives for Hybrid Electric Vehicles

Christopher H.T. Lee, James L. Kirtley, Jr. and
M. Angle

Additional information is available at the end of the chapter

Abstract

Because of the ever-increasing concerns on the energy utilization and environmental protection, the development of hybrid electric vehicles (HEVs) has become a hot research topic. As the major part of HEV technologies, the electric motor drives have to offer high efficiency, high power density, high controllability, wide-speed operating range, and maintenance-free operation. In particular, the switched reluctance (SR) motor drive can achieve most of these goals; therefore, this motor type has drawn much attention in the past. This chapter aims to serve as an overview of the latest developments of the SR motor drive, purposely for HEV applications. To be specific, the discussions on motor structures for torque density enhancement and torque ripple minimization are covered.

Keywords: electric vehicle, hybrid electric vehicle, motor drive, switched reluctance, torque density enhancement, torque ripple minimization

1. Introduction

With ever-enhancing concerns on energy crisis and environmental pollution, as one of the most promising solutions, the development of electric vehicles (EVs) has been speeding up in recent years [1, 2]. However, the traditional EVs are powered by battery as the sole energy source, so that this particular EV type can only provide support for short-duration trips and is not favourable for typical daily drivers [3, 4]. To extend the normal driving range and to relieve the problem, the hybrid electric vehicle (HEV), which incorporates an additional internal combustion engine (ICE) as the supplementary source, has drawn extensive attention in return [5].

As the major component for the HEV systems, the electric motor drives have to fulfil several criteria [6, 7], including

- high efficiency,

- high power and torque densities,

- high controllability,

- wide-speed operating range,

- maintenance-free operation,

- high reliability and robustness,

- high cost-effectiveness.

Since the interior permanent-magnet (IPM) motor drives can achieve most of the desired goals, these types of motor drives have been widely adopted in some famous HEV systems, such as Toyota Prius HEV [8]. Even though the IPM motor drive can offer very desirable power and torque performances for HEV applications, it suffers from the problem of high PM material costs and uncontrollable PM flux densities [9, 10]. Hence, the magnetless switched reluctance (SR) motor drives, which offer satisfactory cost-effectiveness and desirable flux controllability, have become more popular recently [11, 12].

The purpose of this chapter is to serve as an overview of the latest SR motor developments in HEV applications. The current and upcoming design philosophies of the SR motor drives will be discussed. In addition, quantitative comparisons among the latest designs will also be covered.

2. Hybrid electric vehicle architecture

The fundamental HEV can be defined as the vehicle system that consists of two or more power sources, while there are numerous combinations available in the domestic market. Nowadays, the most common HEV architecture includes the electric motor drive and the ICE. In general, the typical HEV system can be classified into two major groups, namely, the series HEV and the parallel HEV, as shown in **Figures 1** and **2**, respectively.

In the series HEV system, the HEV is powered solely by the electric motor drive, while the motor drive can be supplied either from the battery or from ICE-driven generator unit, or even both [3]. On the other hand, in the parallel HEV system, the HEV can be powered by either the electric motor drives or ICE, or by both simultaneously.

In both the series and parallel HEV systems, the battery can be recharged by the ICE during normal operation, so that the battery capacity as well as the battery size can be greatly reduced, as compared with the EV systems. Similar to the EV system, the HEV systems can also offer the regenerative braking operation, such that the battery can be recharged by the electric motor drives when the HEV undergoes braking conditions. As a result, the overall fuel efficiency can be greatly improved, as compared with the standard ICE vehicles.

Since the series HEV relies solely on the motor drive to power the HEV itself, the motor drive is relatively larger and more expensive, as compared with those employed in the parallel HEV
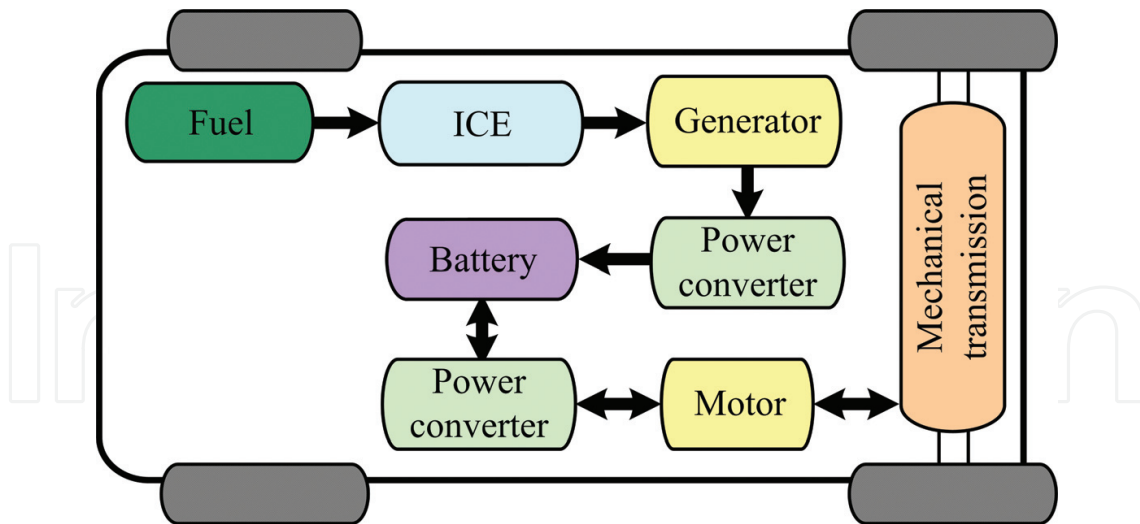
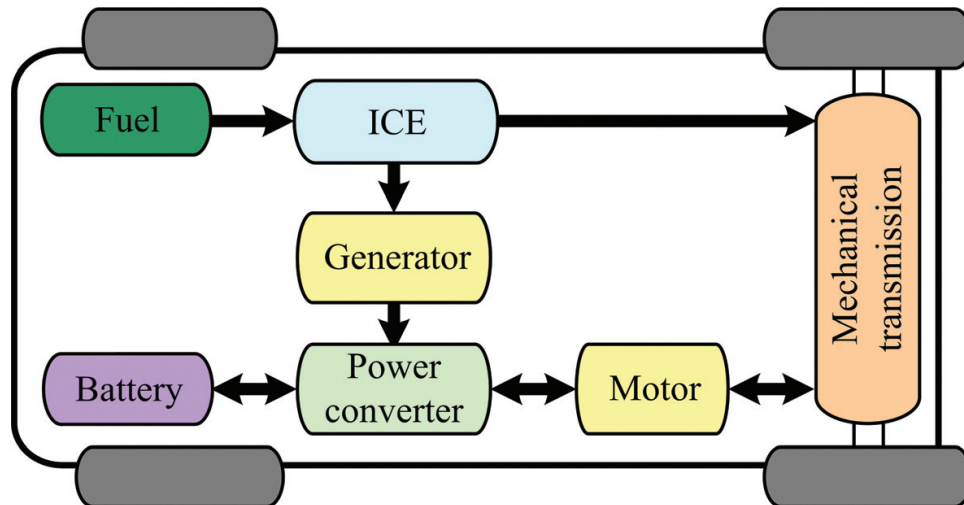**Figure 1.** Series hybrid electric vehicle system.

Figure 2. Parallel hybrid electric vehicle system.

counterparts. On the other hand, the parallel HEV needs not to be powered barely from electric motor drives, so that the motor sizing can be reduced. By taking all the criteria into consideration, the series HEV is generally favourable for specialist applications, while the parallel HEV for broad applications.

3. Switched reluctance motor drives

With the definite advantages of low material cost, robust structure, mature converter topology, high efficiency, satisfactory power and torque densities, and simple control algorithm, the SR motor drives have been considered as a promising candidate for HEV applications. Without any installation of PM material or winding on its rotor, the SR motor drives enjoy the higher

cost-effectiveness and wide-speed operation range, as compared with its counterparts. To be specific, unlike the induction and PM motor drives, SR motor drives can relieve the mechanical problems caused by the centripetal forces at high-speed operation.

The SR motor drives consist of the simple structure, while its design philosophies require sophisticated analysis and researches. Because of the inherited doubly salient topology, the SR motor drives result in nonlinear inductance value, high saturation in pole tips, and severe fringing effect among the poles. All these characteristics increase the design difficulty when the magnetic circuit approach is employed. In general, the finite element method (FEM) is known as the most accurate and convenient tool to analyse the SR motor drives [7]. In this chapter, the commercial FEM software, JMAG-Designer, is adopted for the motor performance analysis. Upon the employment of the FEM-based electromagnetic analysis, the key parameters and performances of the SR motor drives can be provided.

3.1. Stator and rotor pole arrangement

To operate the SR motor drives properly, its stator and rotor poles must obey certain specific regulations. To be specific, the stator and rotor poles should be equally distributed among the circumferences, so that the pole arrangement is governed as

$$\begin{cases} N_s = 2mk \\ N_r = N_s \pm 2k \end{cases} \tag{1}$$

where N_s is the number of stator poles, N_r is the number of rotor poles, m is the number of phases and k is a positive integer. The fundamental pole combination of the SR motor drives is shown in **Table 1**.

To minimize the switching frequency as well as the core losses, the stator poles are generally chosen to be larger than the rotor poles, i.e. $N_s > N_r$ in Eq. (1). A typical example of a three-phase 6/4-pole SR motor drive is shown in **Figure 3**. By taking the reliability and cost-effectiveness into consideration, the three-phase and four-phase SR motor drives are the equally common candidates employed in the domestic markets. The three-phase SR motor drive takes the definite advantage of a larger winding slot area, as compared with the four-phase counterpart. However, with the inherited larger dead zones, the three-phase SR motor drive suffers

m	k	N_s	N_r	N_r
3	1	6	8	4
4	1	8	10	6
5	1	10	12	8
3	2	12	16	8
4	2	16	20	12

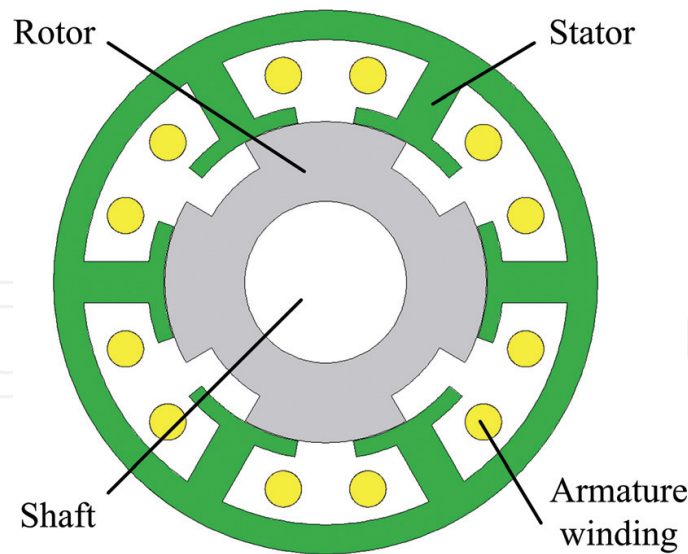**Table 1.** Fundamental pole combinations of switched reluctance motor drives.

Figure 3. Three-phase 6/4-pole switched reluctance motor.

from a larger torque ripple problem. The torque pulsation can be relieved based on the larger number of poles per phase structure, i.e. the three-phase 12/8-pole structure.

3.2. Operating principle

Since the SR motor drives consist of the doubly salient structure, its reluctance of the magnetic flux path varies along the stator-rotor position. The torque can then be produced based on the 'minimum reluctance' rule, i.e. the rotor pole has the tendency to align with the excited stator pole such that the reluctance of the magnetic flux can be minimized.

The operating principle and the theoretical waveform are shown in **Figure 4**. To produce a positive electromagnetic torque T, the armature current i should be injected when the self-inductance L is increasing. The torque production can be described as

$$T = \frac{1}{2} i^2 \frac{dL}{d\theta} \qquad (2)$$

The operating speed n of the SR motor drives is governed by the number of rotor poles N_r and the operating frequency f as

$$n = \frac{60f}{N_r} \qquad (3)$$

In general, the larger the number of rotor poles, the lower the operating speed in the given operating frequency. Therefore, the SR motor drives with a larger number of rotor poles, e.g. the three-phase 12/8-pole and the four-phase 16/12-pole structures, are more preferable for low-speed applications, such as the direct-drive HEV system.
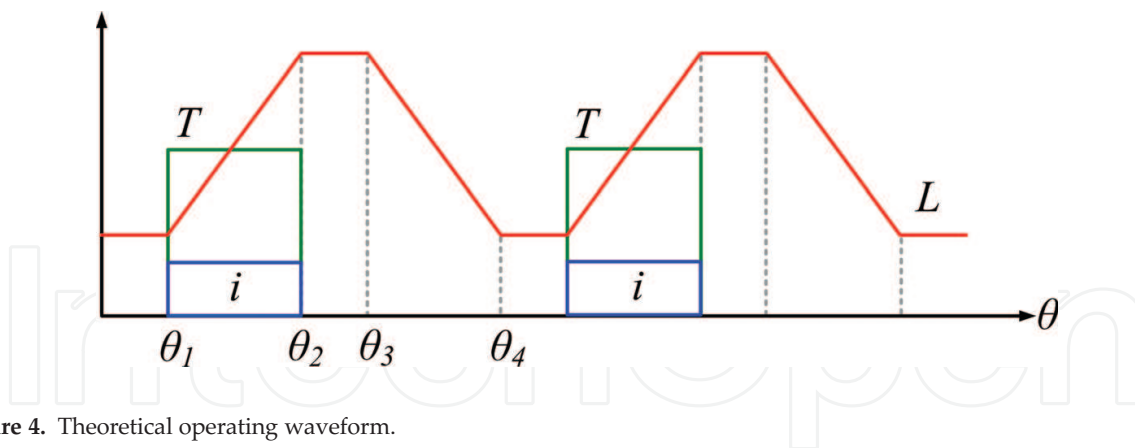
Figure 4. Theoretical operating waveform.

4. Torque density enhancement

4.1. Double-stator structure

As one of the most important criteria for HEV applications, the enhancement of torque density for SR motor drives has become a hot research area. Similar to other commonly employed motor drives, the conventional SR motor drives generally adopt the outer-stator and inner-rotor structure in most occasions. With this traditional topology, the inner spacing of the motor drives is heavily wasted. To improve the situation and to utilize the inner spacing for torque production, the double-stator (DS) topology has been developed [13].

In general cases, the outer and inner segments of the DS motor drives are duplicated, so that both of them employ the same pole arrangement. Since the outer and inner segments are symmetric, the outer and inner armature windings can be connected in series to simplify the operating algorithm. An example of the three-phase 6/4-pole DS-SR motor drive is shown in **Figure 5**. Upon this design, both the outer and inner stators can transfer power to the rotor simultaneously, so that the torque density of the DR motor drives can be greatly improved, as compared with the single-stator counterparts. Because of the additional stator construction, the DS motor drives suffer from higher manufacturing complexity. Yet, the SR motor drives are free from PM material installations, so that the corresponding manufacturing processes are still acceptable and feasible in practical situations.

4.2. Performance analysis of double-stator structure

Based on Eq. (1), the three-phase 12/8-pole single-stator SR motor drive and the three-phase 12/8-pole DS-SR motor drive are designed and are shown in **Figures 6** and **7**, respectively. The three-phase single-stator SR motor consists of the outer-stator and inner-rotor structure, while the three-phase DS-SR motor consists of the dual-stator sandwiched rotor structure. The outer and inner segments of the DS-SR motor are purposely designed with the symmetrical pattern, such that the armature coils can be connected in series. The proposed SR motor drives are designed based on the specification of the typical HEV applications [14], while the key design data are listed in **Table 2**.
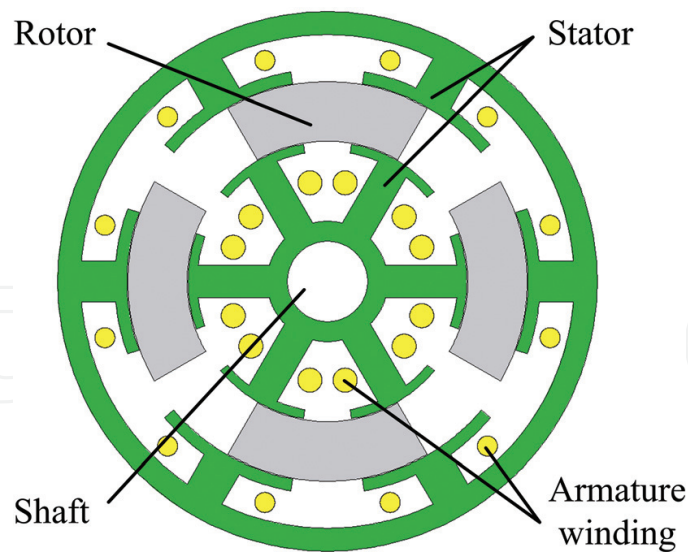
Figure 5. Three-phase 6/4-pole double-stator switched reluctance motor.
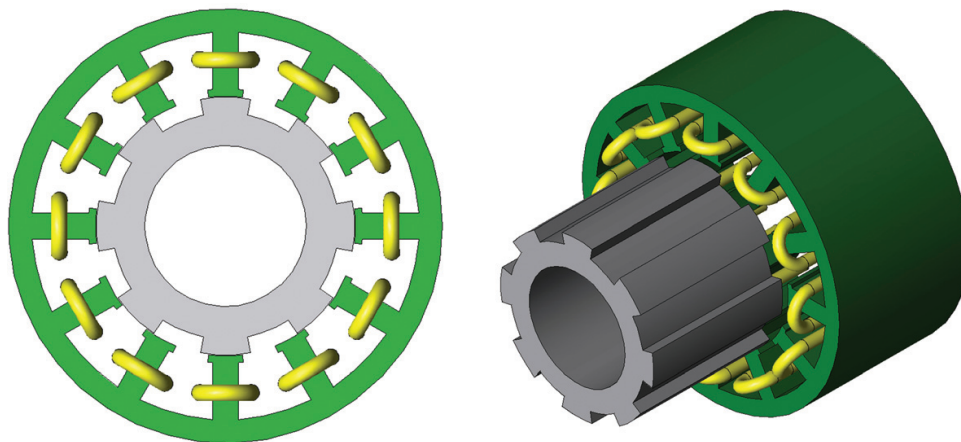

Figure 6. Three-phase 12/8-pole single-stator switched reluctance motor.

To offer a fair comparison, all the key parameters, namely the outer-stator outside diameter, airgap length, stack length, and slot fill factor are set equal. In the meantime, the motor drives are purposely optimized to avoid the magnetic saturation, such that the corresponding core losses can be minimized.

The magnetic field distributions of the SR motor and the DS-SR motor are shown in **Figures 8** and **9**, respectively. As shown, the field distribution of the two proposed motors is well balanced with no obvious saturations. The results somehow give the evidence that the proposed motors are optimized after the iterative approach, in a way their power losses can be minimized. Since the DS-SR motor consists of a symmetrical structure between the outer and the inner segments, the magnetic field distributions between the two segments are also symmetrical.
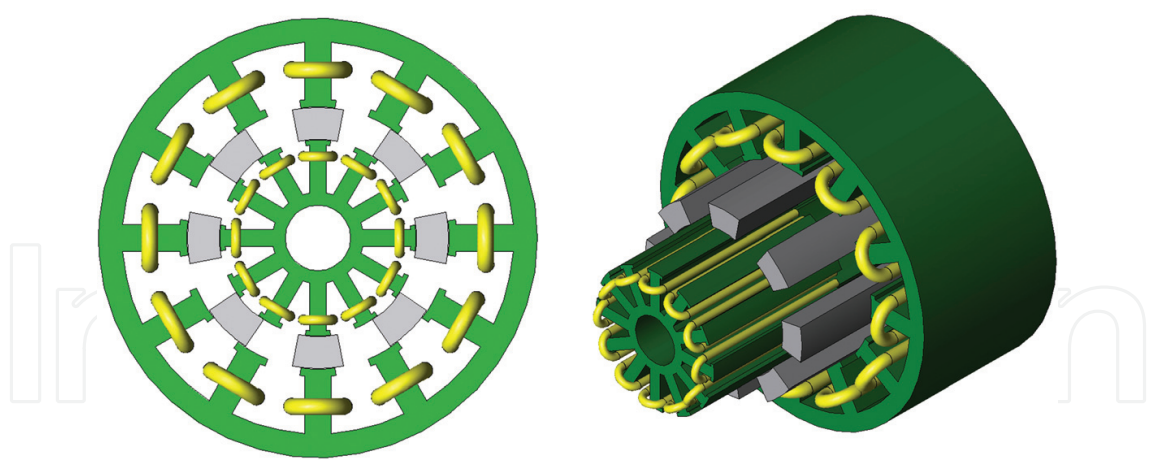
Figure 7. Three-phase 12/8-pole double-stator switched reluctance motor.

Item	SR	DS-SR	MO-DS-SR
Number of stator pole	12	12	12
Number of rotor pole	8	8	8
Outside-stator outside diameter	269 mm	269 mm	269 mm
Outside-stator inside diameter	161 mm	161 mm	161 mm
Rotor outside diameter	160 mm	160 mm	160 mm
Rotor inside diameter	100 mm	121 mm	121 mm
Inside-stator outside diameter	N/A	120 mm	120 mm
Inside-stator inside diameter	N/A	40 mm	40 mm
Airgap length	0.5 mm	0.5 mm	0.5 mm
Stack length	135 mm	135 mm	135 mm
Slot fill factor	55%	55%	55%
Number of phase	3	3	3
Number of outer armature turn	50	50	50
Number of inner armature turn	N/A	18	18
Mechanical offset	0°	0°	60°

Table 2. Key design data of proposed motor drives.

The airgap flux density of the SR motor, the outer airgap density and the inner-airgap density of the DS-SR motor are shown in **Figures 10–12**, respectively. Since the outer and inner segments of the DS-SR motor are symmetrical, as expected, its outer and inner airgaps are symmetrical in nature. In the meantime, not surprisingly, the single stator and DS-SR motor share the same flux patterns because both of them share the same motor structure and operating principle.
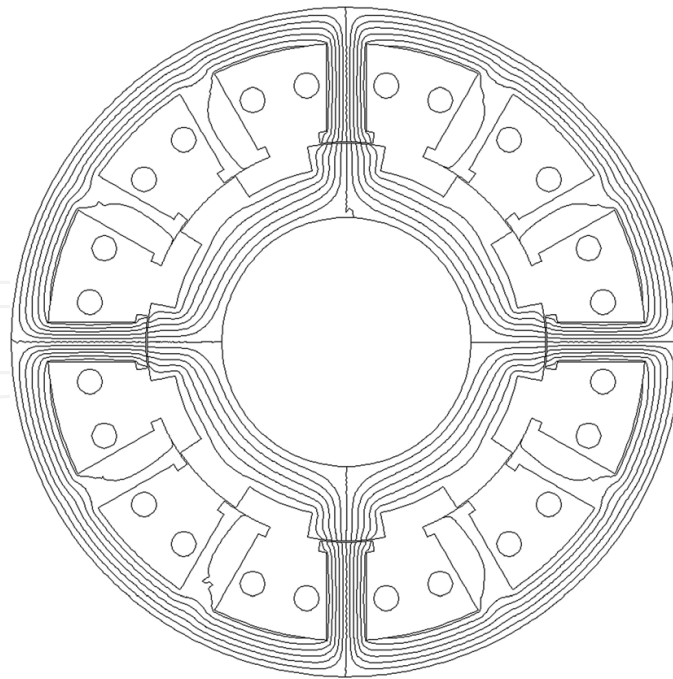
Figure 8. Magnetic field distribution of the switched reluctance motor.
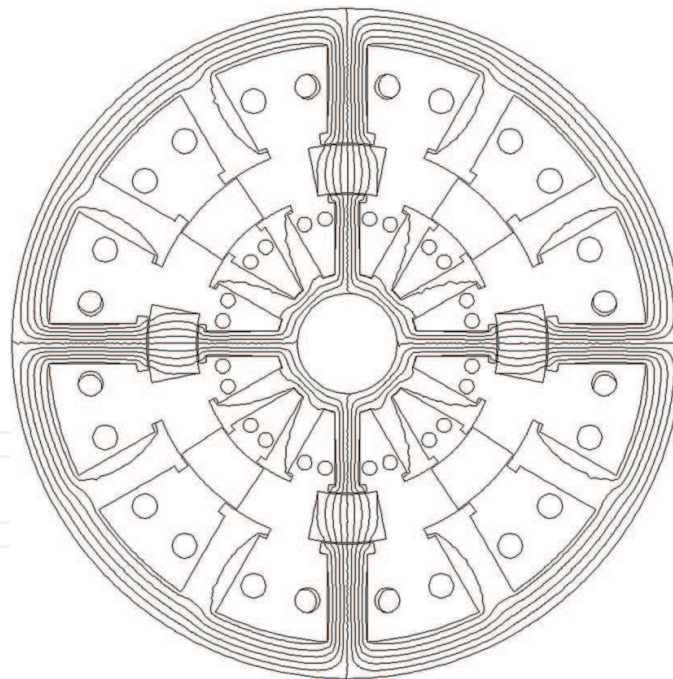

Figure 9. Magnetic field distribution of the double-stator switched reluctance motor.

The torque capabilities of the SR motor and the DS-SR motor are given in **Figures 13** and **14**, respectively. The motor drives are conducted with various armature currents from 50 to 200 Å with a step of 50 Å. The torque capabilities of both motors follow the description from Eq. (2),
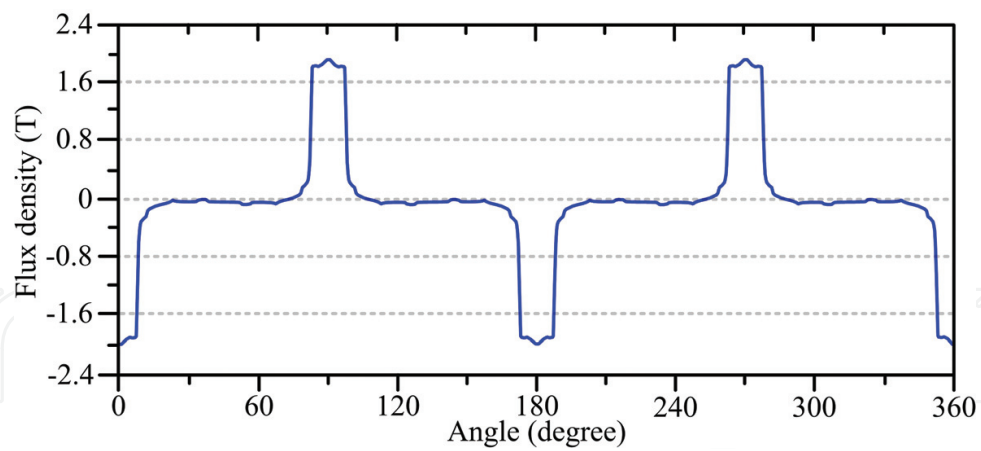
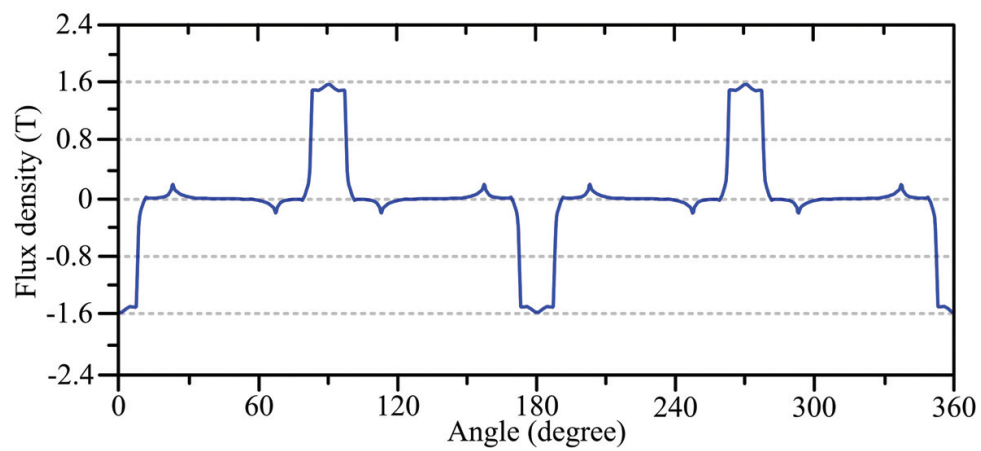**Figure 10.** Airgap flux density of the switched reluctance motor.

Figure 11. Outer-airgap flux density of the double-stator switched reluctance motor.
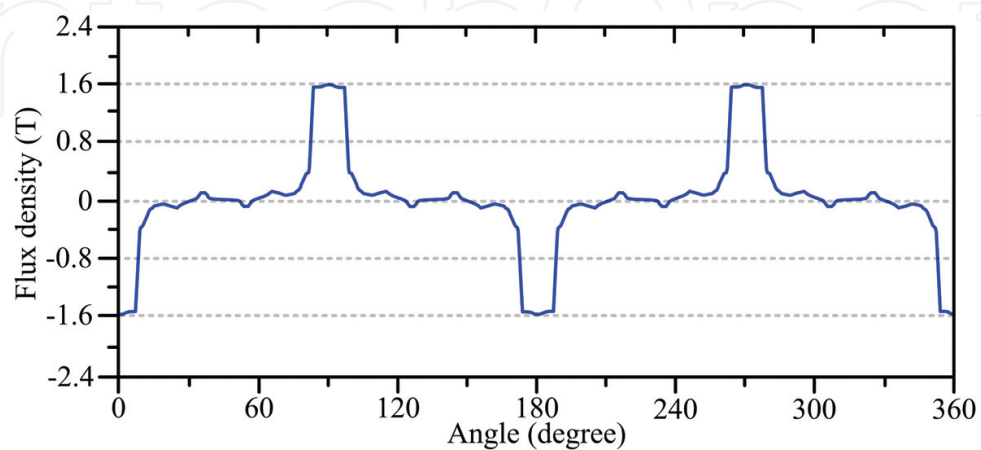

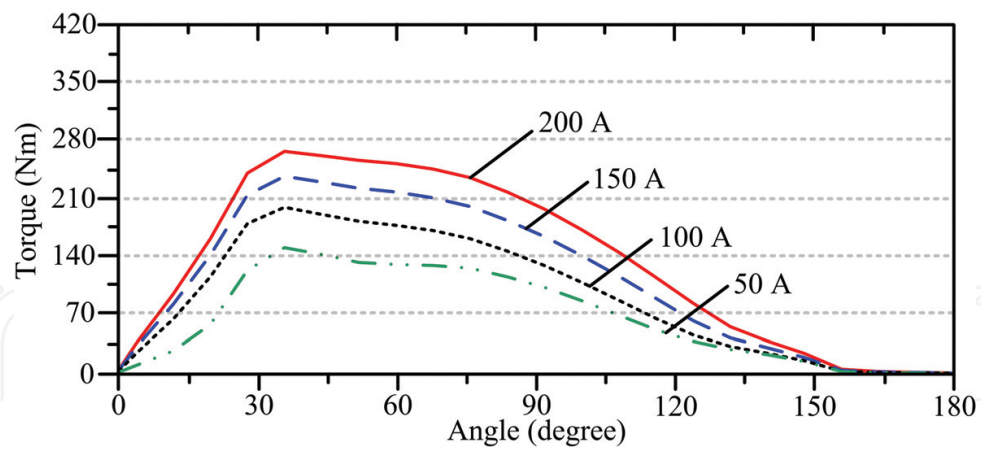**Figure 12.** Inner-airgap flux density of the double-stator switched reluctance motor.

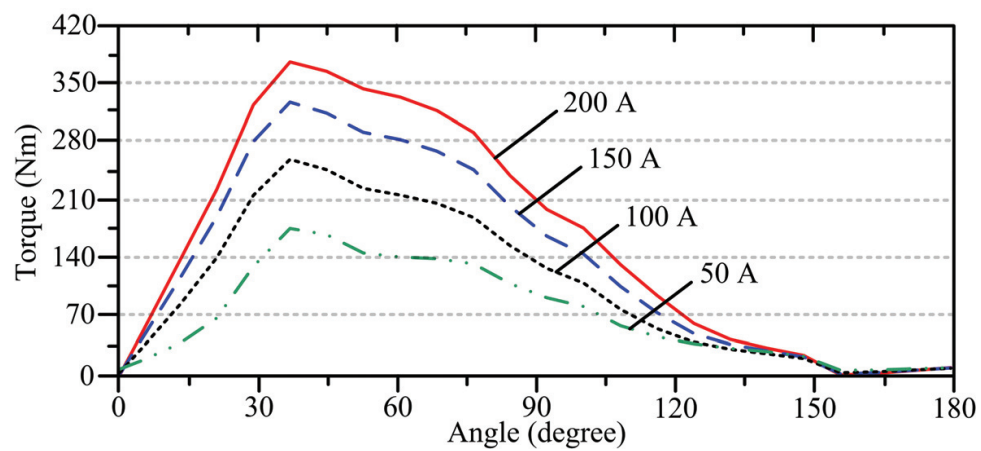**Figure 13.** Torque capabilities of the switched reluctance motor.

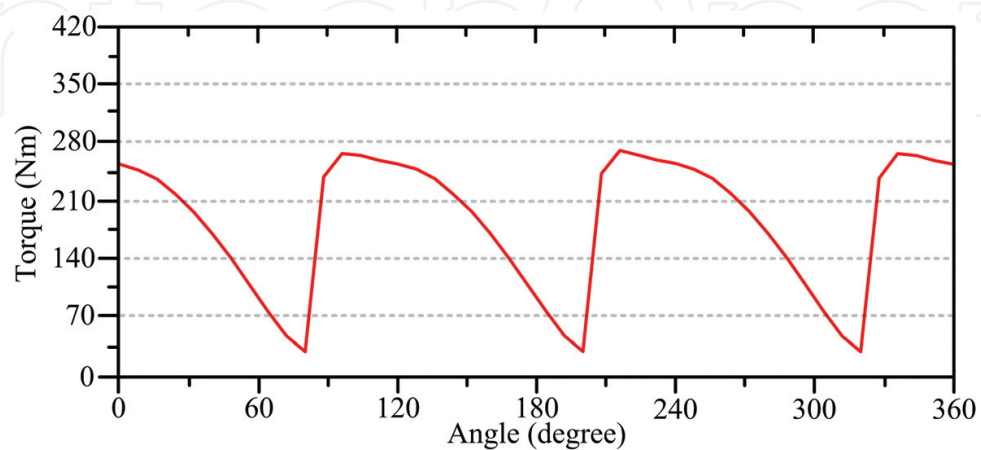**Figure 14.** Torque capabilities of the double-stator switched reluctance motor.

Figure 15. Steady torque waveform of the switched reluctance motor.

such that it can be confirmed that the proposed motors consist of a minimized magnetic saturation problem. In addition, it can also be confirmed that with the DS structure, the DS-SR motor can produce higher torque capability than its single-stator counterpart.

The steady output torques of the SR and the DS-SR motors are given in **Figures 15** and **16**, respectively. As shown, the average torque of the SR motor is about 178 Nm, while of the DS-SR motor is 242 Nm. The torque enhancement from the DS structure can be up to 36%. The performance comparisons between the two proposed motors, namely, the single-stator SR motor and the DS-SR motor are summarized in **Table 3**.
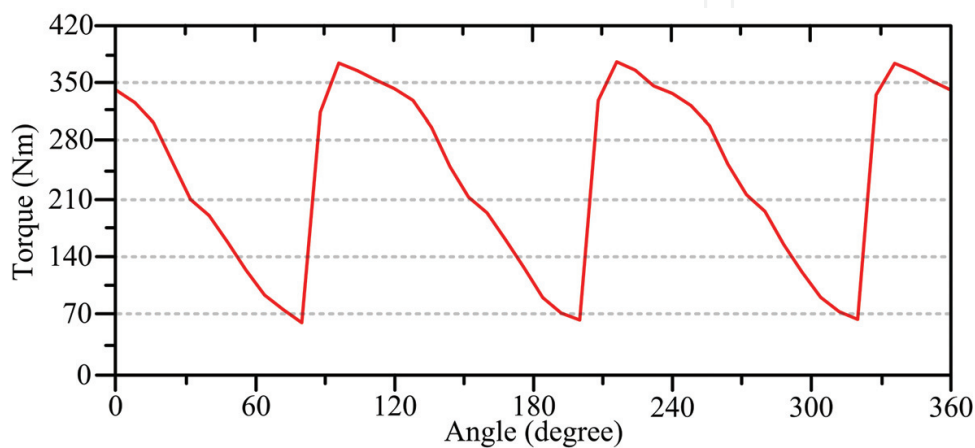

Figure 16. Steady torque waveform of the double-stator switched reluctance motor.

Item	SR	DS-SR
Rated power	22 kW	30 kW
Base speed	1200 rpm	1200 rpm
Outer-airgap flux density	1.9 T	1.6 T
Inner-airgap flux density	N/A	1.6 T
Rated torque	178 Nm	242 Nm
Torque enhancement	N/A	36%

Table 3. Performance comparisons between the torque density enhancement structures.

5. Torque ripple minimization

5.1. Mechanical-offset structure

The DS structures can definitely improve the torque densities, while the torque ripple value, another key criterion to determine the torque performance, should also be discussed. The torque vibration in the SR motor drives can be explained from the torque production processes, i.e. the

torque pulsation generated by the commutation between different phases. To quantitatively analyse the torque ripple performance, the torque ripple factor K_T is widely employed as

$$K_T = \frac{T_{max} - T_{min}}{T_{avg}} \times 100\% \tag{4}$$

where T_{max}, T_{min}, and T_{avg} are the maximum, minimu and average torque produced, respectively.

According to Eq. (4), the torque pulsation value is inversely related to the average torque value, so that mathematically the torque ripple can be reduced upon the increase of average torque. As aforementioned, the conventional DS motor drives generally employ the symmetrical structure between the outer and inner segments, such that the outer and inner rotor teeth are aligned with each other. Upon this arrangement, the local maxima and local minima of the torque ripples from the outer and inner segments are unfavourably integrated, such that the increased torque level can barely benefit the torque ripple value.

On the other hand, the mechanical-offset (MO) structure, which purposely mismatches the outer and inner rotor teeth with a conjugated angle to each other, can greatly improve the torque pulsation problem [15]. Upon the MO structure, the local torque ripple maxima and local minima from the outer and inner segments are favourably offset with each other, such that the torque ripple problem can be relieved.

5.2. Conduction algorithm for conventional double-stator motor drive

As described in Section 3.2, to produce an electromagnetic torque, a unipolar rectangular armature current should be injected in accordance with the status of the self-inductance with conduction angle $\theta_c = \theta_2 - \theta_1$, as further elaborated in **Figure 17**. Since the conventional DS motor drive employs the symmetrical structure between its outer and inner segments, the armature windings in the outer and inner stators of the conventional DS motor drive are connected in series. Consequently, to operate the motor drive properly, the armature currents in both stators are identical as
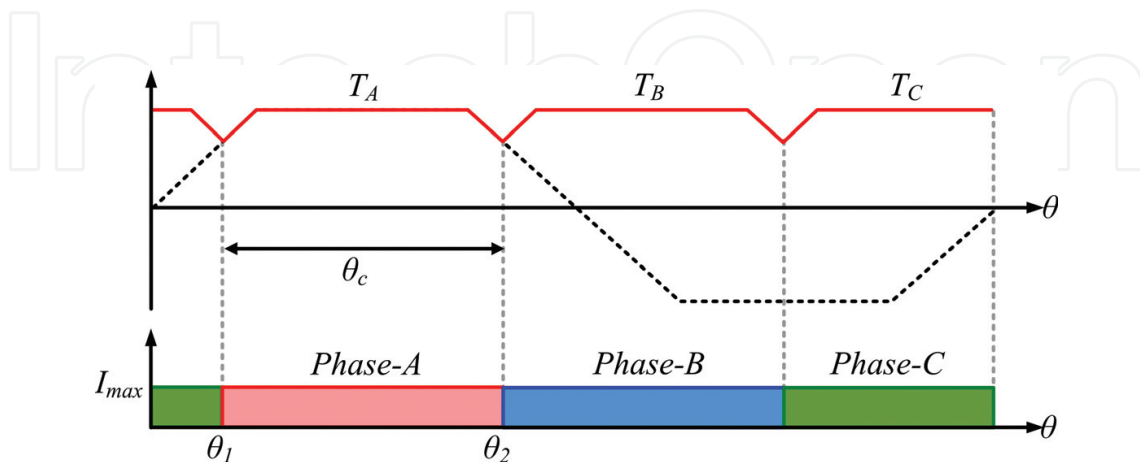

Figure 17. Operating principle for switched reluctance motor.

$$\begin{cases} i_k = I_{\max}\ \theta_1 \le \theta \le \theta_2 \\ i_k = 0\ 0 < \theta < \theta_1,\ \theta_2 < \theta < 2\pi \end{cases} \quad \text{for } k = 1,\ 2 \tag{5}$$

where i_1 and i_2 are the armature windings in the outer and inner stators, respectively. Using this conduction algorithm, as shown in **Figure 18**, the power from both stators can be transferred to the rotor simultaneously, so that the torque density of the DS motor can be boosted. However, the local maxima and local minima of the two individual torque components are unfavourably integrated with each other. As a result, the torque ripple value remains the same, as compared with the single-stator counterpart.

5.3. Conduction algorithm for mechanical-offset motor drive

As described in Eq. (2), the average torque magnitude is governed by the relative position between the stator and rotor teeth. Consequently, the local maxima and local minima of the torque ripple are also governed by the relative position between the stator and rotor teeth. Upon the MO structure, the outer and inner rotor teeth of the SR motor drive are artfully mismatched with a conjugated electrical angle of $\theta_m = \pi/m$, as shown in **Figure 19**. Since the outer and inner rotor teeth no longer align with each other, the armature currents in the two stators should be operated separately. To be specific, either one set of the armature winding should be injected with current described in Eq. (5), while the other set as follows

$$\begin{cases} i_{1\ or\ 2} = I_{\max}\ \theta_1 + \theta_m \le \theta \le \theta_2 + \theta_m \\ i_{1\ or\ 2} = 0\ \theta_m < \theta < \theta_1 + \theta_m,\ \theta_2 + \theta_m < \theta < 2\pi + \theta_m \end{cases} \tag{6}$$

Upon this conduction scheme, the local maxima and local minima of the torque ripples are artfully offset with each other, so that the torque pulsations generated by the two torque components can be favourably compensated. As a result, the smoother resultant torque, as compared with those produced by the conventional DS motor drives, can be generated.
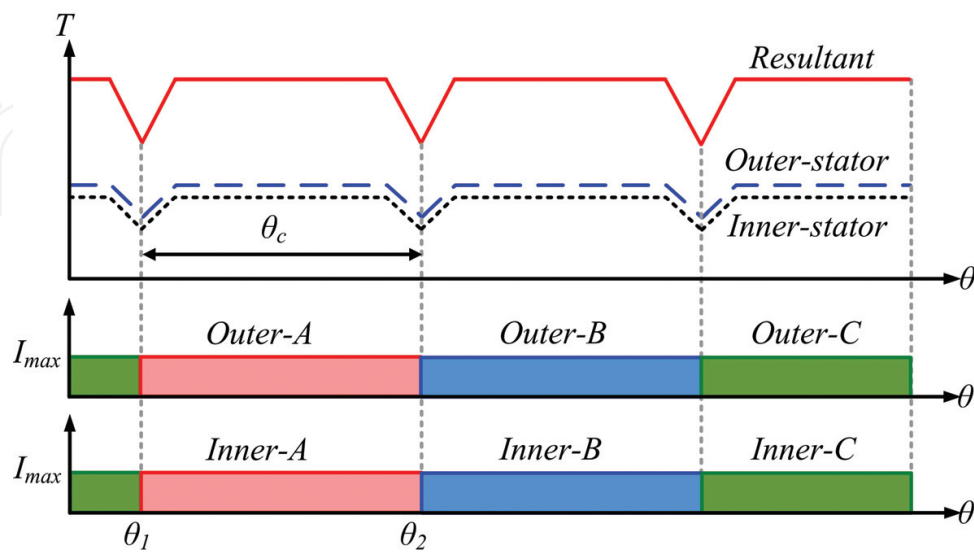

Figure 18. Operating principle for conventional double-stator switched reluctance motor.
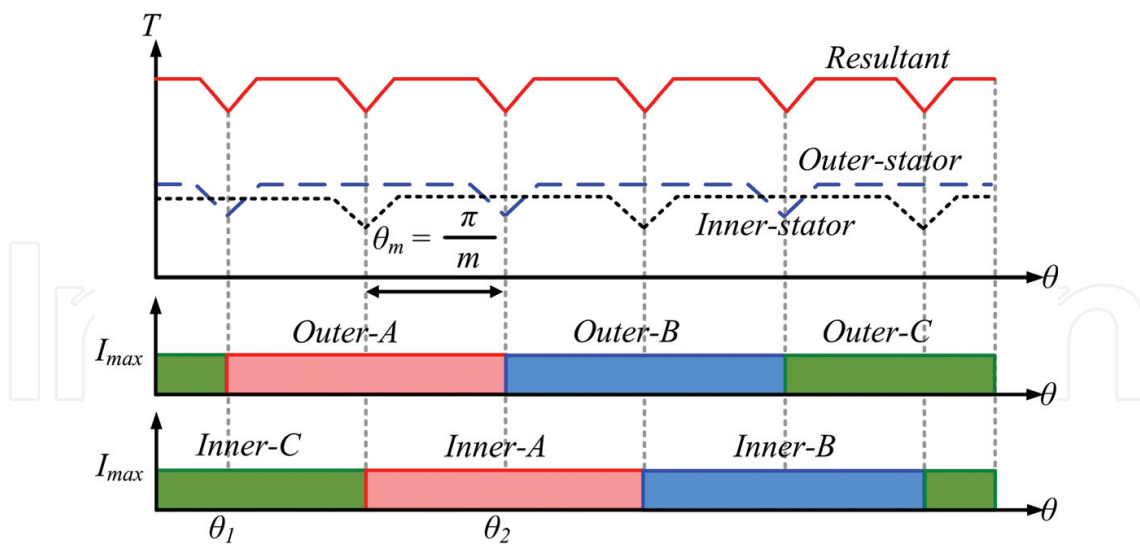
Figure 19. Operating principle for mechanical-offset double-stator switched reluctance motor.

5.4. Torque characteristics of the mechanical-offset motor drive

Since the two torque components of the MO motor drive are integrated with each other, in principle, its resultant torque level should not be affected. Therefore, the MO motor drive should be able to produce the same torque level, as compared with the conventional DS counterpart. To offer a better torque ripple minimization effect, the magnitudes between the two torque components should be adjusted to similar levels. This can be handled by modifying the design of the motor dimensions, i.e. the electric loadings between the outer and inner segments, which are out of scope of this chapter.

Unlike the DS motor drives that align the local torque ripple maxima and local minima together, the MO motor drive purposely mismatches these torque ripples. As a result, the local maxima and local minima are spread according to the conjugated position, such that the pulsating frequency is double, as compared with the DS counterpart.

5.5. Performance analysis of mechanical-offset structure

Based on Eq. (1), the three-phase 12/8-pole MO-DS-SR motor drive is designed and shown in **Figure 20**. To offer a fair comparison, the MO-DS-SR motor is purposely designed based on the same conditions in Section 4.2. Both the DS-SR motor and the MO-DS-SR motor share the same motor structure, while the major distinction comes from the rotor alignments, i.e. the outer and inner rotor teeth of the DS-SR motor align with each other, while those of the MO-DS-SR motor are purposely mismatched with a conjugated angle. The key design data of the MO-DS-SR motor are listed in **Table 2**.

The steady torques of the DS-SR motor and the MO-DS-SR motor are shown in **Figures 21** and **22**, respectively. The average rated torque of the outer-stator, the inner-stator, and both stators of the DS-SR motor are 178, 68, and 242 Nm, respectively, while those of the MO-DS-SR motor are 178, 68, and 239 Nm, respectively. It can be confirmed that the two torque components of the MO-DS-SR

motor are seamlessly integrated with each other, so that the same torque level, as compared with the DS-SR counterpart, can be produced. With the MO structure, the local torque ripple maxima and local minima are favourably offset with each other, so that the MO-DS-SR motor can reduce its
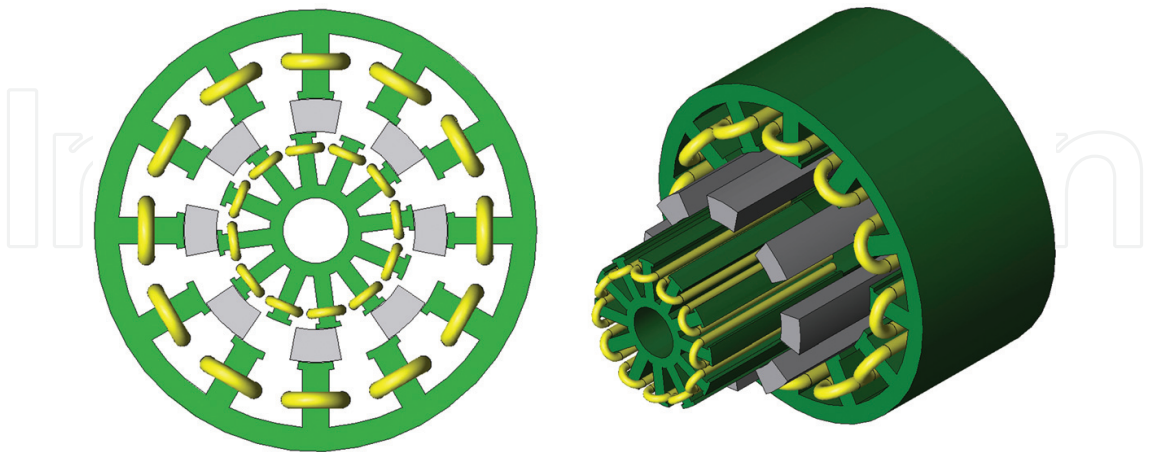

Figure 20. Three-phase 12/8-pole mechanical-offset double-stator switched reluctance motor.
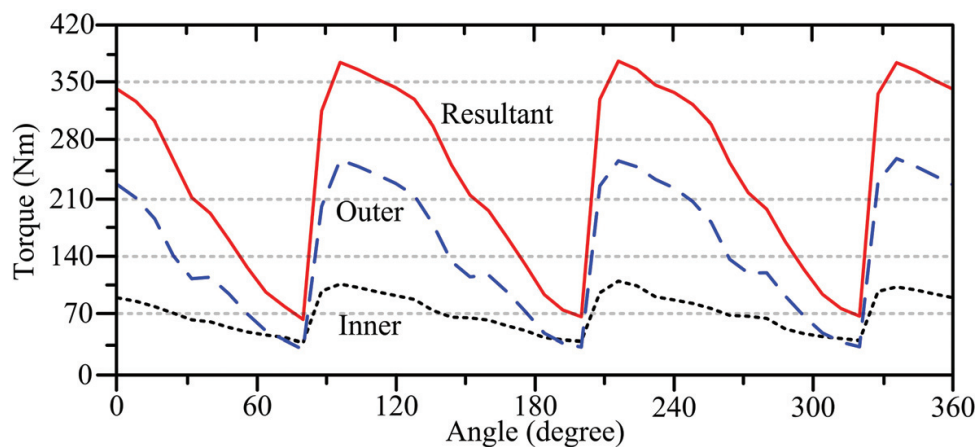

Figure 21. Steady torque waveforms of the conventional double-stator switched reluctance motor.
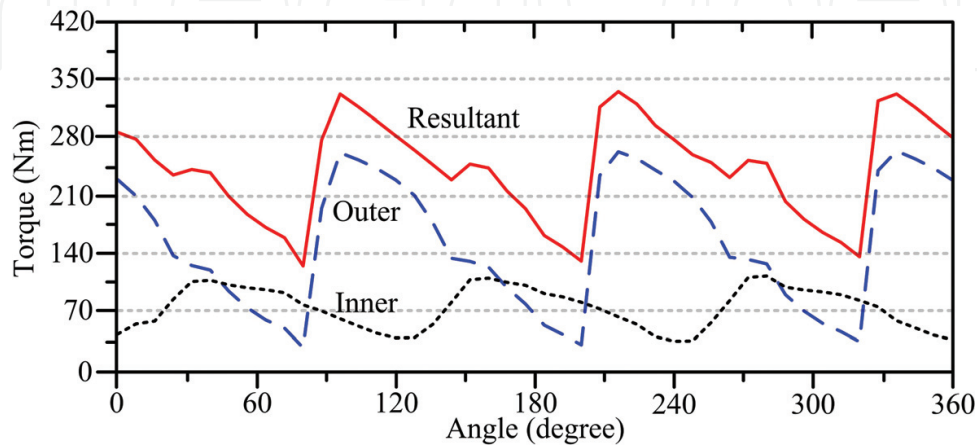

Figure 22. Steady torque waveforms of the mechanical-offset double-stator switched reluctance motor.

Item	DS-SR	MO-DS-SR
Rated power	30 kW	30 kW
Base speed	1200 rpm	1200 rpm
Outer-stator torque	178 Nm	178 Nm
Inner-stator-torque	68 Nm	68 Nm
Resultant torque	242 Nm	239 Nm
Torque ripple	124%	81%

Table 4. Performance comparisons between the torque ripple minimization structures.

torque ripple value to 81%, as compared with those of 124% in the DS-SR motor. The performance comparisons among the two proposed motors, namely, the DS-SR motor and the MO-DS-SR motor are summarized in **Table 4**.

6. Conclusion

In this chapter, the design criteria, principles of operation, and the key performances of the SR motor drives are carefully discussed and quantitatively compared, based on the fair conditions. To be specific, the torque density enhancement structure, namely the DS structure, and the torque ripple minimization structure, namely the MO structure, are included. This chapter provides the latest research trend on SR motor drives for HEV applications, such that it can serve as the blueprint and start-up manual for the potential readers to develop the research interests in this particular area.

Author details

Christopher H.T. Lee*, James L. Kirtley, Jr. and M. Angle

*Address all correspondence to: chtlee@mit.edu

Research Laboratory of Electronics, Massachusetts Institute of Technology, Cambridge, Massachusetts, United States

References

[1] Chan CC. The state of the art of electric, hybrid, and fuel cell vehicles. Proceedings of the IEEE. 2007;**95**(4):704–718

[2] Emadi A, Lee YJ, Rajashekara K. Power electronics and motor drives in electric, hybrid electric, and plug-in hybrid electric vehicles. IEEE Transactions on Industrial Electronics. 2008;**55**(6):2237–2245

[3]   Ehsani M, Gao Y, Gay SE, Emadi A. Modern Electric, Hybrid Electric, and Fuel Cell Vehicle. Boca Raton, FL: CRC Press; 2004

[4]   Zhu ZQ, Howe D. Electrical machines and drives for electric, hybrid, and fuel cell vehicles. Proceedings of the IEEE. 2007;**95**(4):746–765

[5]   Lee CHT, Liu C, Chau KT. A magnetless axial-flux machine for range-extended electric vehicles. Energies. 2014;**7**(3):1483–1499

[6]   Cheng M, Hua W, Zhang J, Zhao W. Overview of stator-permanent magnet brushless machines. IEEE Transactions on Industrial Electronics. 2011;**58**(11):5087–5101.

[7]   Chau KT. Electric Vehicle Machines and Drives: Design, Analysis and Application. Singapore: Wiley-IEEE Press; 2015

[8]   Cao R, Mi C, Cheng M. Quantitative comparison of flux-switching permanent-magnet motors with Interior permanent magnet motor for EV, HEV, and PHEV applications. IEEE Transactions on Magnetics. 2008;**48**(8):2274–2384

[9]   Boldea I, Tutelea LN, Parsa L, Dorrell D. Automotive electric propulsion systems with reduced or no permanent magnets: An overview. IEEE Transactions on Industrial. Electronics. 2014;**61**(10):5696–5711

[10] Lee CHT, Chau KT, Liu C. Design and analysis of an electronic-geared magnetless machine for electric vehicles. IEEE Transactions on Industrial. Electronics. 2016;**63**(11):6705–6714

[11] Rahman KM, Fahimi B, Suresh G, Rajarathnam AV, Ehsani E. Advantages of switched reluctance motor applications to EV and HEV: Design and control issues. IEEE Transactions on Industry Applications. 2000;**36**(1):111–121

[12] Chiba A, Takano Y, Takeno M, Imakawa T, Hoshi N, Takemoto M, Ogasawara S. Torque density and efficiency improvements of a switched reluctance motor without rare-earth switched reluctance motor without rare-earth. IEEE Transactions on Industry Applications. 2011;**47**(3):1240–1246

[13] Abbasian M, Moallem M, Fahimi B. Double-stator switched reluctance machines (DSSRM): Fundamentals and magnetic force analysis. IEEE Transactions on Energy Conversion. 2010;**25**(3):589–597

[14] Takeno M, Chiba A, Hoshi N, Ogasawara S, Takemoto M, Rahman MA. Test results and torque improvement of the 50-kW switched reluctance motor designed for hybrid electric vehicles. IEEE Transaction on Industry Applications. 2012;**48**(4):1327–1334

[15] Lee CHT, Chau KT, Liu C, Ching TW, Li F. Mechanical offset for torque ripple reduction for magnetless double-stator doubly salient machine. IEEE Transactions on Magnetics. 2014;**50**(11):8103304